Molecular Psychiatry (2014), 1–8

www.nature.com/mp

ORIGINAL ARTICLE

Astrocyte pathology in the prefrontal cortex impairs the cognitive function of rats

A Lima[1,2], VM Sardinha[1,2], AF Oliveira[1,2], M Reis[1,2], C Mota[1,2], MA Silva[1,2], F Marques[1,2], JJ Cerqueira[1,2], L Pinto[1,2], N Sousa[1,2] and JF Oliveira[1,2]

Interest in astroglial cells is rising due to recent findings supporting dynamic neuron–astrocyte interactions. There is increasing evidence of astrocytic dysfunction in several brain disorders such as depression, schizophrenia or bipolar disorder; importantly these pathologies are characterized by the involvement of the prefrontal cortex and by significant cognitive impairments. Here, to model astrocyte pathology, we injected animals with the astrocyte specific toxin L-α-aminoadipate (L-AA) in the medial prefrontal cortex (mPFC); a behavioral and structural characterization two and six days after the injection was performed. Behavioral data shows that the astrocyte pathology in the mPFC affects the attentional set-shifting, the working memory and the reversal learning functions. Histological analysis of brain sections of the L-AA-injected animals revealed a pronounced loss of astrocytes in the targeted region. Interestingly, analysis of neurons in the lesion sites showed a progressive neuronal loss that was accompanied with dendritic atrophy in the surviving neurons. These results suggest that the L-AA-induced astrocytic loss in the mPFC triggers subsequent neuronal damage leading to cognitive impairment in tasks depending on the integrity of this brain region. These findings are of relevance to better understand the pathophysiological mechanisms underlying disorders that involve astrocytic loss/dysfunction in the PFC.

Molecular Psychiatry advance online publication, 14 January 2014; doi:10.1038/mp.2013.182

Keywords: aminoadipate; astrocyte; cognition; learning; prefrontal cortex

INTRODUCTION

The knowledge of the nervous system has evolved rapidly in the last decades, namely due to the disclosure of more prominent role of astrocytes in physiological and pathological processes. Among glial cells, astrocytes were pointed out as neuronal partners since they keep a concerted cross-talk with vicinal neurons, which is crucial for normal brain function. Astrocytes are able to sense neuronal activity by expressing an extensive number of neurotransmitter receptors, which lead to both homeostatic changes and cellular cross-talk.[1,2] The astrocytic homeostatic responses include alterations of metabolic activity, synthesis of neuronal preferred energy substrate lactate, clearance of neurotransmitters and buffering of extracellular K^+ ions.[1,3,4] With respect to the alterations of cellular cross-talk, a bidirectional communication between neurons and astrocytes, conceptualized as the tripartite synapse,[5–7] was extensively demonstrated both in brain slice preparations[8–16] and *in vivo*[17–24] in rodents and, more recently, in humans.[25]

Taking these evidences into account, it is expected that changes in astrocyte number and/or function would impact on the neuron-astrocyte network integrity and activity and, consequently, on behavior output. Indeed, a large set of evidence has pointed out an important pathological role of astrocytic dysfunction in several conditions.[26–28] In particular, specific astrocytic markers such as the glial fibrilary acidic protein (GFAP) or glutamine synthetase were shown to be decreased in the context of brain disorders such as depression, schizophrenia or bipolar disorder,[29–40] consisting a state of astrocyte pathology possibly having a role on its pathophysiology.[41–44] Amongst the most affected brain regions is the prefrontal cortex (PFC),[26,30,32,34] which is implicated in attentional processes, decision-making, goal-directed behavior, working memory, processing of emotional stimuli, temporal organization of behavior, rule learning and behavior flexibility.[45–48] Furthermore, the medial prefrontal cortex (mPFC) is anatomically and functionally linked with other components of the limbic system, which justifies the key role in cognitive, mnesic and emotional processing.[49,50] Accordingly, astrocyte loss in the PFC is sufficient to induce depression-like behavior in the rat[51–53] and blockade of astrocytic glutamate uptake in this region is also sufficient to produce anhedonia, a hallmark of depression.[54]

Although these observations may also justify the cognitive dysfunction observed in patients suffering mood disorders the impact of astrocyte loss in the mPFC, and consecutively on mPFC-dependent cognitive function is still poorly understood. In order to tackle this question, we induced an astrocyte pathology state in the mPFC by injection of the specific astrocyte toxin L-aminoadipate and assessed cognitive function of the treated animals by testing their performance in working memory, behavior flexibility, attention and reference memory tasks, as well as by characterizing the structural consequences of astrocytic loss in the mPFC.

MATERIALS AND METHODS

Animals and treatments

Experiments were conducted in accordance with local regulations (European Union Directive 86/609/EEC) and National Institutes of Health guidelines on animal care and experimentation. Male Wistar-Han rats (Charles River Laboratories, Barcelona, Spain), ten-weeks-old, were housed

[1]Life and Health Sciences Research Institute (ICVS), School of Health Sciences, University of Minho, Braga, Portugal and [2]ICVS/3B's—PT Government Associate Laboratory, Braga/Guimarães, Portugal. Correspondence: Dr JF Oliveira, Life and Health Sciences Research Institute (ICVS), School of Health Sciences, University of Minho, Campus de Gualtar, 4710-057 Braga, Portugal.
E-mail: joaooliveira@ecsaude.uminho.pt
Received 2 August 2013; revised 8 November 2013; accepted 12 November 2013

in groups of two, under standard laboratory conditions (room temperature 22 °C; food and water *ad libitum*; 12 h dark/light cycle, lights on at 08:00). The astrocyte pathology model was obtained by the intracranial injection of the selective toxin L-α-aminoadipate (L-AA)[55] in treated animals. The two groups of animals used for experimentation, control (CON) and treated (AA), were obtained by a single bilateral microinjection of artificial cerebrospinal fluid (aCSF) or L-AA, respectively, in the mPFC. In order to avoid interference of the injection surgical procedures with the behavior performance, cannula guides were surgically implanted in all animals one week prior to the microinjection. The injections took place one day before the start of the experiment through the implanted cannulas with minor impact to the animal. Detailed surgical and injection procedures are given in SI.

Behavioral testing

The consequences of the induced astrocyte pathology in the mPFC to the cognitive function of CON and AA animals were assessed in the attentional set-shifting task (ASST) and in water maze tests. Animals of CON and AA groups were divided into two sub-sets. The first sub-set performed two days of ASST and the second sub-set performed six days of water maze tests. Therefore, the tests were performed within the effect window of the toxin previously described.[55]

The ASST was used to assess the non-spatial working memory, the attentional set-shifting and the reversal learning functions of rats based on previously described protocols.[56] Briefly, the test was conducted in a rectangular arena (black Plexiglass; 60 cm × 40 cm × 20 cm) where animals were required to dig and find a reward (Nestlé Cheerios® cut in two) in one of two bowls filled with sawdust. The reward was related to the presence of relevant odor or texture stimuli that were randomly exchanged (for test scheme, Figure 1a; Supplementary Table S1), being the criterion accomplished whenever six consecutive correct responses were achieved for each stage.

Water maze tests were used to assess the performance of experimental animals in spatial working and reference memory tasks as described previously.[57,58] Briefly, these tests were conducted in a circular black pool (170 cm diameter) filled with water at 22 °C to a depth of 34 cm in a room with extrinsic clues (triangle, square, cross and horizontal stripes) and dim light. An invisible platform was placed in one of four quadrants as observed in Figures 2a and d. In the working memory task (WMT), animals had to learn the location of the hidden platform and to retain this information online during the four consecutive trials since the platform was placed in a different position each day. In the reference memory task (RMT), the platform position was unchanged. Distances swam and escape latencies to platform were used as readout of task performance. Details on the behavior tasks are given in SI. After the last day of behavior testing, all animals were sacrificed and brain tissue was collected.

Histological analysis

In order to analyze the histological implications of the injection of aCSF or L-AA, we performed the immunohistochemical characterization of frozen coronal sections (20 µm thick) containing the mPFC of five CON and four L-AA animals that performed the ASST and six CON and eight L-AA animals that performed the water maze tests (for methodological details, see SI). Briefly, brain sections were stained for: GFAP (astrocytes; 1:200, DakoCytomation, Glostrup, Denmark), NeuN (neurons, 1:100, Millipore, Schwalbach, Germany) and DAPI (nuclei, 1:1000, Invitrogen, Paisley, UK); GFAP (astrocytes; 1:200, DakoCytomation), S100β (astrocytes, 1:100, Sigma, Taufkirchen, Germany) and DAPI (nuclei, 1:1000, Invitrogen); S100β (astrocytes, 1:100, Sigma) with 3,3-diaminobenzidine (DAB); GFAP (astrocytes; 1:200, DakoCytomation), Iba1 (microglia, 1:100, Abcam, Cambridge, UK) and DAPI (nuclei, 1:1000, Invitrogen). The effect of L-AA injection in the mPFC was evaluated by analyzing the numbers of GFAP- and NeuN-positive cells (to assess the effect on astrocytes and neurons, respectively) in the targeted region dorsal PrL/Cg1 (lesion site), and in the ventral PrL, (peri-lesion site; see results section) through confocal microscopy imaging (FV1000, Olympus, Hamburg, Germany) and ImageJ software (http://rsbweb.nih.gov/ij/). The density of cells, given in number of cells per μm^2, in lesion and peri-lesion sites was normalized to the density of cells in the infralimbic (IL—a neighbor unaffected area) of the same brain section. The resulting relative values allowed comparison between different animals excluding variation due to fluctuation of staining quality between sections.

To further understand the consequences of L-AA injection to neurons of the affected areas, their three-dimensional dendritic morphology was analyzed and compared to the site of aCSF infusion, in CON animals.

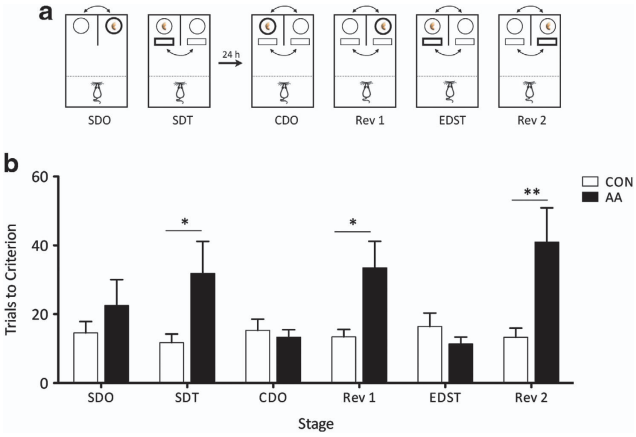

Figure 1. Astrocyte pathology in the mPFC impairs attentional set-shifting and reversal learning in the ASST. (**a**) Scheme of test stages: SDO—simple discrimination by odors, SDT—simple discrimination by textures, CDO—compound discrimination by odors, Rev 1—CDO reversal, EDST—extradimensional shift textures, Rev 2—EDST reversal; (**b**) Trials to reach criterion of rats injected with aCSF (CON, white) and L-AA (AA, black); Data plotted as mean ± s.e.m. $*P < 0.05$, $**P < 0.01$.

Neuronal structures were also analyzed in the IL region of animals in both groups to confirm that changes were restricted to the affected area. Briefly, the analysis was performed for ten neurons in each region for each animal group in coronal brain slices after Golgi-Cox impregnation.[59] Identification and reconstruction of Golgi-impregnated layer III pyramidal neurons in the mPFC and estimation of spine densities was performed as previously described.[59] Dendritic trees were reconstructed using a motorized microscope (Axioplan 2, Carl Zeiss, Göttingen, Germany) and Neurolucida/NeuroExplorer software (Microbrightfield, Williston, VT, USA). To assess structural changes, number of basal dendrites, total length and branches of basal and apical trees, as well as Sholl analysis[60,61] were compared across groups. For spine density analysis, dendritic segments of 30 µm were randomly selected in the proximal and distal portions of the apical dendrite and basal dendrites, and spines were classified in mushroom, thin, wide and ramified categories. For details on the histological procedures and neuronal reconstruction, see SI.

Statistical analysis

Data are expressed throughout the manuscript as means ± s.e.m. Statistical analysis was performed using the Prism 5 (GraphPad Software Inc., La Jolla, CA, USA). Unpaired *t*-test was applied to compare: dendritic length; number of branches or dendrites; total spine density. Two-way analysis of variance (ANOVA) analysis and Bonferroni *post-hoc* tests were applied to analyze: ASST and water maze task performances; cell counts between lesion and non-lesion sites; dendritic length or number of intersections of neurons in the Sholl analysis; densities of the four categories of spines. The statistical significance of the comparisons for each statistical test was set with a confidence interval of 95%.

RESULTS

The results presented in this section represent all animals on which the bilateral injections of aCSF (CON group) or L-α-aminoadipate (AA group) targeted the mPFC (Supplementary Figure S1; see histological results below). Therefore, the data herein presented enclose behavior outputs of seven CON and six AA animals that performed ASST, and six CON animals and eight AA that performed water maze tests.

Astrocyte pathology in the mPFC impairs the working memory and reversal learning functions of rats

In order to assess the translation of astrocyte loss in the behavior output of the mPFC, animals injected with the toxin L-AA and their

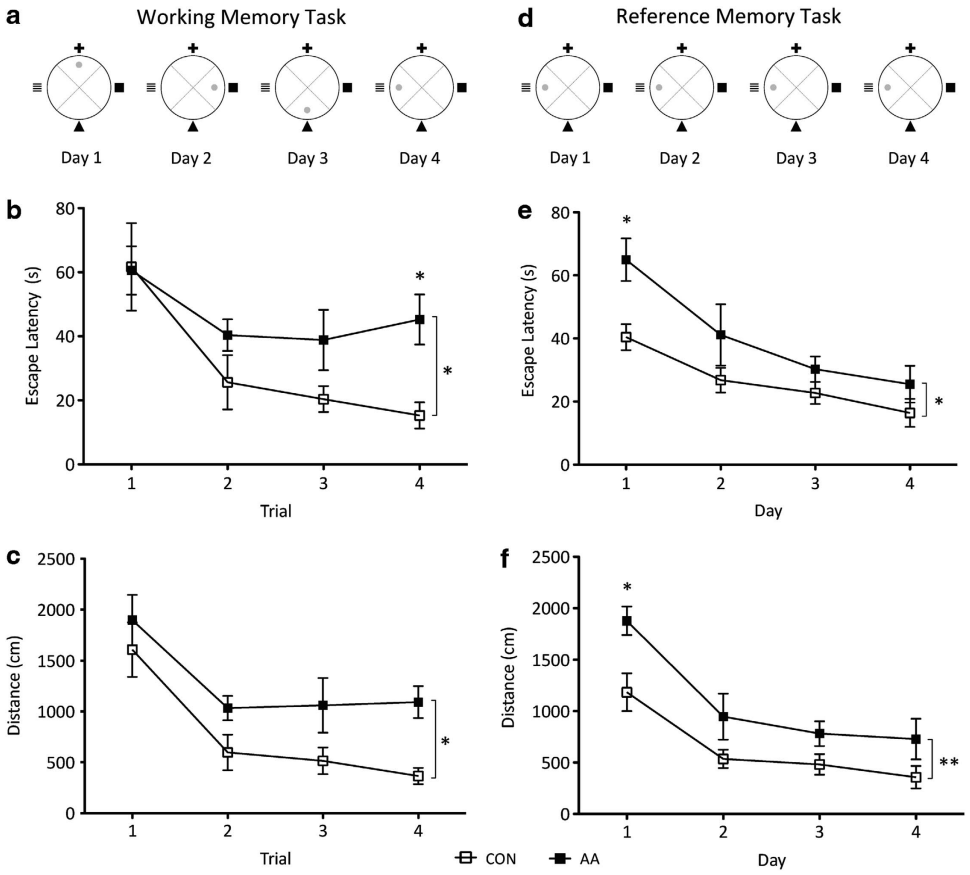

Figure 2. Astrocyte pathology in the mPFC impairs working memory in the water maze. (**a**) Test scheme for the working memory task, WMT; (**b**) Escape latencies and (**c**) distances swam in the WMT; (**d**) Test scheme for the reference memory task, RMT; (**e**) Escape latencies and (**f**) distances swam in the RMT. Rats injected with aCSF (CON, white) and L-AA (AA, black). Data plotted as mean ± s.e.m. $*P < 0.05$, $**P < 0.01$.

respective controls performed tasks dependent on the function of this region.

The ASST (Figure 1) assesses functions such as attention, dimensional set-shifting and reversal learning.[56] Both controls (CON) and treated animals (AA) animals learnt to discriminate the reward by odor in the first stage of the test since they display a similar number of trials to acquire the rule (trials to criterion, TC; simple discrimination by odor (SDO), $t = 1.1$, $P > 0.05$). However, animals with astrocyte pathology in the mPFC (AA) displayed a striking difficulty in learning to discriminate stimuli in the dimension of textures simple discrimination by textures (SDT, $t = 2.7$, $P < 0.05$) and to perform reversal learning (observed consistently across the stages; Rev 1: $t = 3.0$, $P < 0.05$; Rev 2, $t = 3.8$, $P < 0.01$), when compared to CON (Figure 1b). No differences were observed between groups in the remaining stages (compound discrimination of odors (CDO), $t = 0.2$, $P > 0.05$; or extra dimensional shift of textures (EDST), $t = 0.7$, $P > 0.05$).

The water maze tests were performed to assess spatial working memory (WMT) and spatial reference memory (RMT)[58] in the animals with mPFC astrocyte pathology and respective controls. The analysis of the WMT learning curve showed that astrocyte depletion impaired consistently the working memory (Figure 2b; $F_{1,12} = 5.07$, $P = 0.04$), particularly in trial 4 (trial 1, $t = 0.10$, $P > 0.05$; trial 2, $t = 1.28$, $P > 0.05$; trial 3, $t = 1.61$, $P > 0.05$; trial 4, $t = 2.61$, $P < 0.05$). In the spatial RMT, differences were observed in the learning curves (Figure 2e; $F_{1,12} = 6.85$, $P = 0.03$), mostly due to the acquisition difficulties faced by the AA animals. Differences in distance swam consistently supported the measurements of escape latencies both for WMT (Figure 2c; $F_{1,12} = 8.44$, $P = 0.01$) and RMT (Figure 2f; $F_{1,12} = 9.93$, $P = 0.01$).

L-AA-induced astrocyte pathology is characterized by depletion and neuronal damage in the region affected

The preliminary analysis of the brain sections containing the mPFC of CON and AA animals selected for analysis revealed that the injections targeted specifically an area concerning the dorsal portion of the PrL and Cg1 sub-regions of the mPFC (Supplementary Figure S1). This observation was confirmed by the microscopic analysis of the brain sections stained with GFAP antibody, for AA animals. A fluorescence halo was observed in the sites where the bilateral injection of L-AA took place, on which the GFAP staining was completely absent (Figure 3a). This observation was confirmed by immunostaining with S100β antibody that marked typical astrocyte morphologies, which were absent at lesion sites (Supplementary Figure S2), confirming that L-AA injections lead to the ablation of astrocytes of both GFAP+ and S100B+ populations.

The double staining with astrocytic (GFAP) and neuronal (NeuN) markers revealed that despite the complete absence of astrocytes in the lesion site, neurons were easily observable within this area (Figures 3b and c). The calculation of astrocyte relative densities in lesion areas (given by the number of GFAP+ astrocytes per unit of area, relatively to the density of astrocytes in the IL region of the same section) revealed astrocyte depletion in the L-AA-injected subjects, 2 days post injection ($t = 11.92$, $P < 0.001$; Figure 3d) and 6 days post injection ($t = 8.0$, $P < 0.001$; Figure 3e), when compared to the respective aCSF-injected controls (for absolute values, see Supplementary Table S2). Furthermore, the effects of L-AA were confined to the injection targets, since astrocyte numbers were not affected in the peri-lesion region from any of the tested animals (2 days post injection: $t = 0.34$, $P > 0.05$; Figure 3f; 6 days post injection: $t = 0.57$, $P > 0.05$; Figure 3g).

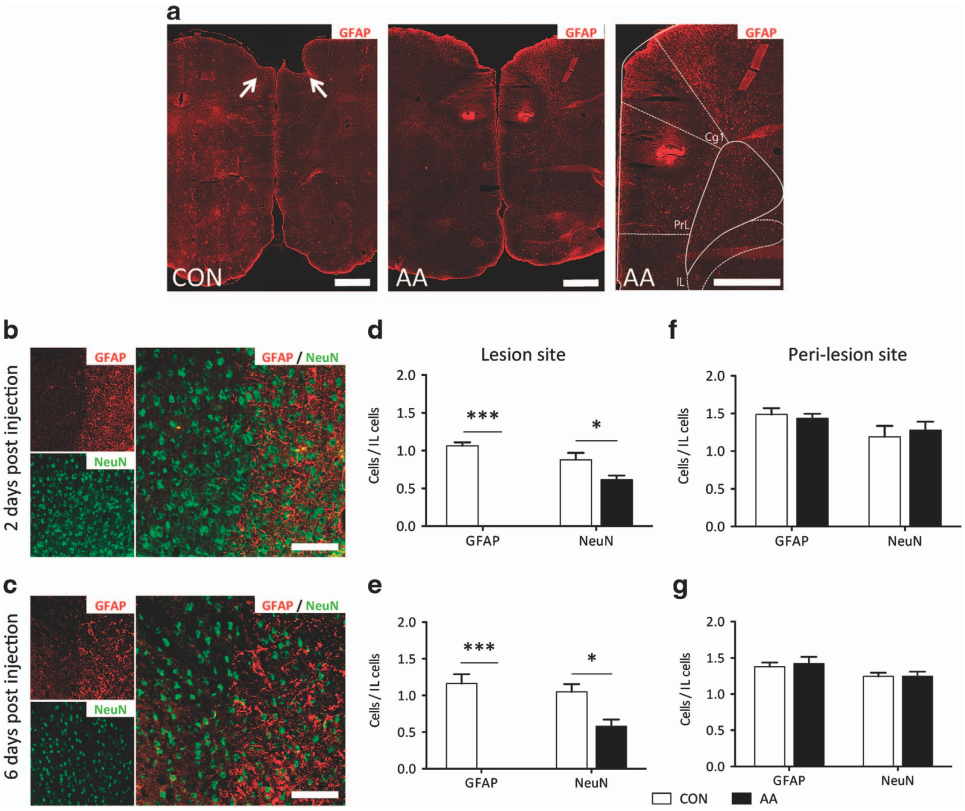

Figure 3. Injection of L-AA induces a defined astrocyte depletion and neuronal damage in the mPFC. (**a**) Representative micrographs of GFAP stained brain sections obtained 2 days post injection; L-AA injections cause astrocyte ablation denoted by nonfluorescent halos in the GFAP immunoreactivity; CON—brain section from control animal; arrows denote the physical damage caused by the cannula placement; AA left—brain section from AA animal evidencing astrocyte ablation in Cg and dorsal PrL, detailed in AA right. (**b** and **c**) Representative confocal images of the lateral lesion border within the PrL region, in brain slices containing the mPFC of AA animals collected 2 and 6 days after injection. (**d** and **e**) Relative numbers of cells within lesion sites (Cg1 and dorsal portion of PrL) over the number of cells in non-lesion region (IL) compared to a peri-lesion (ventral PrL) at 2 (**d**–**f**) and 6 days after injection (**e**–**g**). Scale bars A = 1 mm; B,C = 100 μm. Data plotted as mean ± s.e.m. $*P < 0.05$; $***P < 0.001$.

Interestingly, the calculation of relative neuronal densities (given by the number of NeuN+ neurons per unit of area, relatively to the density of neurons in the IL region of the same section) revealed a 29.9% of neuronal loss in the sites of L-AA injection 2 days ($t = 2.97$, $P < 0.05$; Figure 3d); this loss was considerably higher 6 days post injection (44.8% of loss: $t = 3.3$, $P < 0.05$; Figure 3e), when compared to aCSF-injected controls (for absolute values, see Supplementary Table S2). Again, this effect was restricted to the lesion site as in the vicinity of the lesion, the neuronal densities remained unaltered 2 days ($t = 0.57$, $P > 0.05$; Figure 3f) and 6 days post injection ($t = 0.5$, $P > 0.05$; Figure 3g).

The surgical procedure and injection of saline in control animals did not trigger microglial response, confirmed by the typical resting state morphology with small somas, and fine, long and ramified processes[62] observed at the targeted sites (Supplementary Figures S3A and B). The astrocyte toxin L-AA induced an activation of microglia characterized by alteration of the cell structure, reduction of process length towards an amoeboid structure,[62] which is visible at both 2 and 6 days post injection in the lesion sites (Supplementary Figures S3C and D). These alterations are in line and may explain the structural changes observed in neurons and astrocytes. Regarding the functional consequence of microglial activation, we believe that it may have an impact on the overall activity of the network. However, due to the difficulty to tackle this implication and the controversy on the link between astrocyte loss and microglia activation in psychiatric disorders[63] this issue needs to be further addressed by other studies in the field.

3D neuronal structure in the mPFC is affected by the astrocyte pathology

Regarding the analysis of the neuronal morphology (Figure 4 and Supplementary Figure S4), neurons located at the lesion site of animals from CON and AA groups displayed a quite similar structure 2 days post injection (Figure 4a). Specifically, there were no significant differences in apical dendritic length ($t = 1.35$ $P > 0.05$), number of apical dendrite branches ($t = 1.03$, $P > 0.05$), number of basal dendrite branches ($t = 0.9$, $P > 0.05$) or number of basal dendrites ($t = 0.62$, $P > 0.05$) (Figures 4a and Supplementary Figure S5A); however, a reduction in basal dendritic length was observed in AA-injected animals ($t = 2.34$, $P < 0.05$) (Figure 4a). These observations were similar to those made in the peri-lesion area where no differences between CON and AA animals were observed in any of the parameters estimated (Figure 4c and Supplementary Figure S5C).

Interestingly, the neuronal structure of AA animals in the lesioned areas 6 days post injection was severely affected when compared to CON animals (Figure 4b and Supplementary Figure S5B). Layer III pyramidal neurons of those regions presented reduced apical dendritic length ($t = 4.7$, $P < 0.001$) basal dendritic length ($t = 6.3$, $P < 0.001$; Figure 4b). Interestingly, the number of basal dendrites in neurons in lesion areas of AA animals did not change when compared to the CON group ($t = 0.8$, $P > 0.05$; Figure 4b), which indicates that the reductions in length and branching observed represent atrophy of the existing dendrites, rather than general structure damage. Again, this effect was confined to the lesion area as confirmed by the analysis of 3D

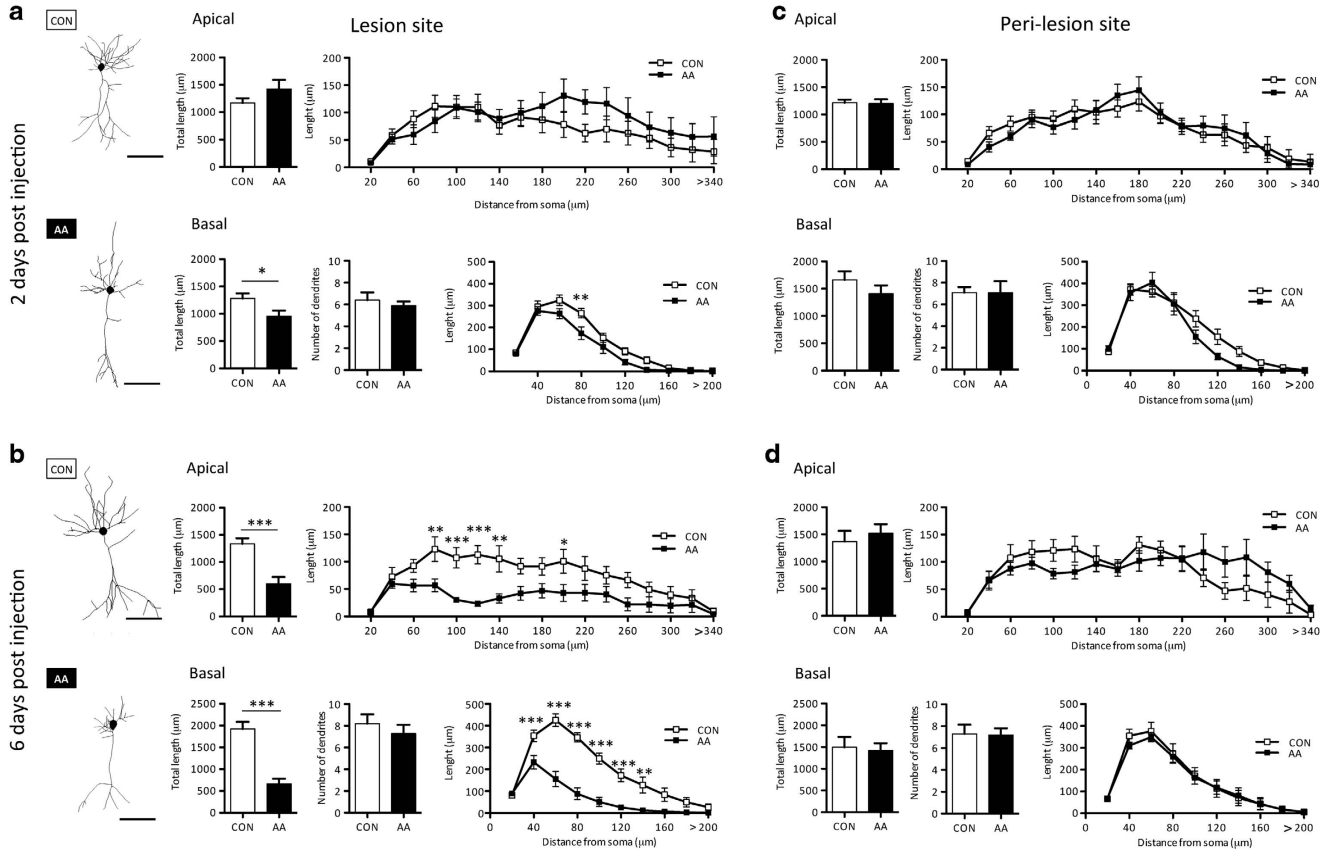

Figure 4. Injection of L-AA induces a progressive damage of dendritic structure in mPFC pyramidal neurons. Analysis of 3D structure of neurons in lesion and peri-lesion sites at 2 (**a** and **c**) and 6 (**b** and **d**) days post injection of aCSF (CON) or L-AA (AA); Each panel: above, mean values ± s.e.m. of total apical dendritic length and Sholl analysis of apical dendrites; below, total basal dendritic length, number of basal dendrites and Sholl analysis of basal dendrites. $^{*}P < 0.05$; $^{**}P < 0.01$; $^{***}P < 0.001$; **a** and **b** left panel, representative 3D reconstructions of neurons of each group. Scale bar = 100 µm.

neuronal structures in the IL, a neighbor area spared from the L-AA injection effects. Here, no significant differences were found in any of the parameters estimated (Figure 4d and Supplementary Figure S5D).

These observations were confirmed by the Sholl analysis that calculates both number of intersections and length of dendrites at specific distances from the soma (Figure 4 and Supplementary Figure S5) both for 2 and 6 days after the lesion. The reorganization of the dendritic material described above is visible in Figures 4a and b left panel (details in Supplementary Figure S4), where representative 3D reconstructions are presented for illustration of treatment effects.

The categorization of spines and determination of its density in basal, apical proximal and apical distal segments of the reconstructed neurons provided a more detailed insight of the effects of astrocyte ablation to the neuronal integrity and function. The absence of astrocytes in targeted regions did not alter the density of spines in basal, apical proximal or apical distal dendritic portions. These observations were true for neurons located within lesion sites from animals 2 days post injection (Figure 5a) and 6 days post injection (Figure 5b). Accordingly, the total density of spines remained intact at peri-lesioned region (IL) as well, either 2 (Figure 5c) or 6 (Figure 5d) days post injection, both in CON and AA groups. The discrimination and quantification of each spine type according to maturity criteria (thin, mushroom, ramified or wide) sustained these observations, since no differences were observed between groups for each spine type between lesion and peri-lesion areas whatsoever (Supplementary Figure S6).

DISCUSSION

The first highlight of this study is the regional specificity of the lesion. In fact, the model used herein allowed to target specifically astrocytes within the mPFC, without signs of lesion in the surrounding areas, at least as indicated by the unaffected astrocytic densities observed at peri-lesion sites. Accordingly, neuronal loss or effects on the dendritic structure were confined to the regions where astrocyte loss occurred. Interestingly, both neuronal loss and dendritic atrophy were increasing with time after the injection of the astrocyte toxin L-AA. This observation was not described previously in similar studies,[51,53,55] a fact that could be ascribed to the technical differences between studies. Since L-AA is described to affect specifically astrocytes and to cause immediate astrocyte loss in the targeted region,[51,53,55] a finding herein confirmed after 2 days of lesion, these pieces of evidence suggest that neuronal damage is as a consequence of the astrocyte loss in the targeted region. In this context of astrocyte pathology, neuronal damage may occur due to the lack of extracellular space homeostasis, excitatory neurotransmitter uptake and metabolic support functions largely attributed to astrocytes that are responsible for the neuronal nourishing, maintenance and survival.[1,2] In particular, lack of astrocytic buffering of extracellular excitatory neurotransmitter glutamate was shown to induce dendritic atrophy[64] and neuronal death through excitotoxicity,[65–67] that are similar to the effects observed in this model of astrocyte pathology.

Typically the L-AA-induced loss of astrocytes targeted the dorsal portion of the prelimbic, as well as the cingulate subregions of the

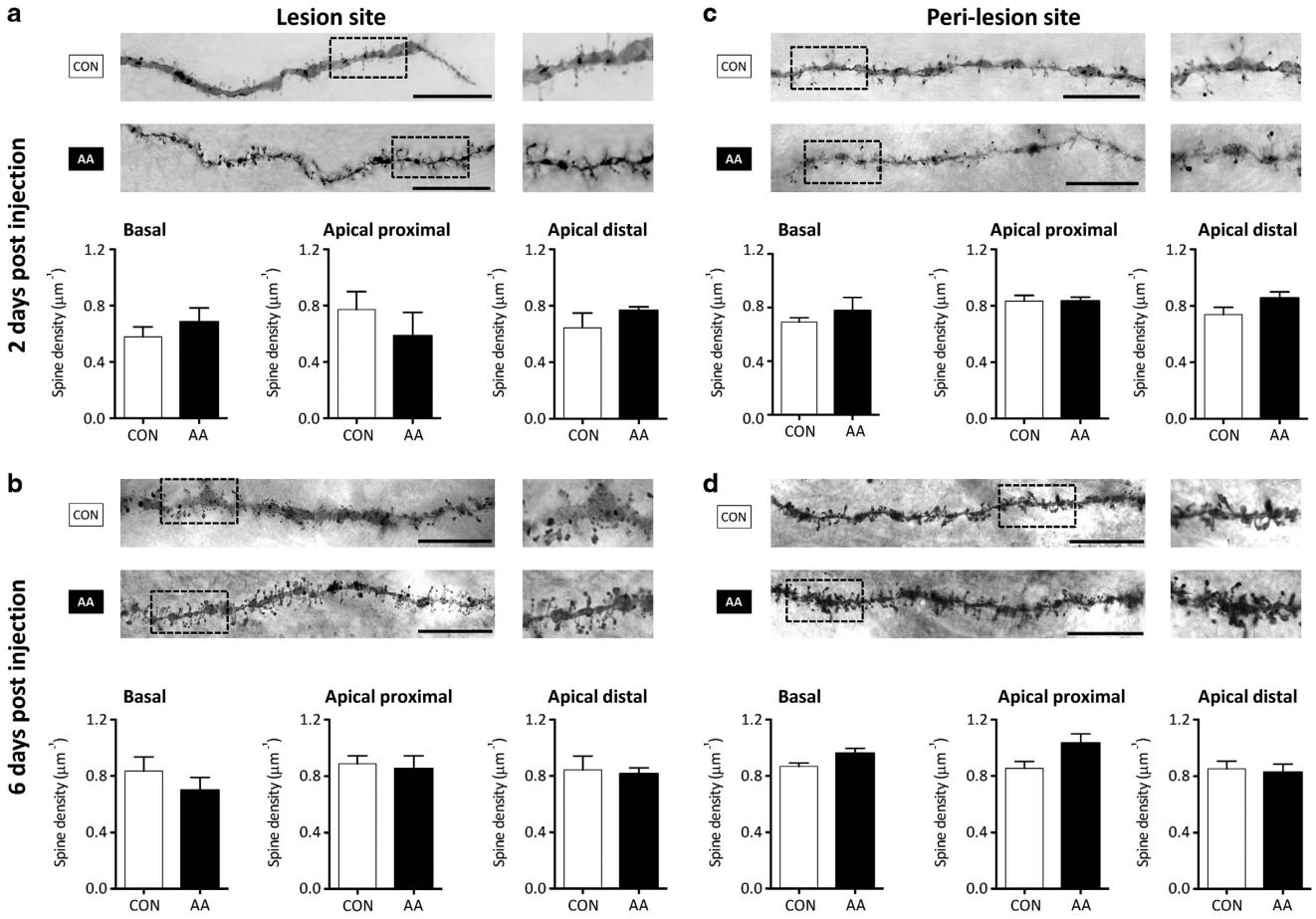

Figure 5. Injection of L-AA does not affect spine density in mPFC pyramidal neurons. High-magnification micrographs of representative dendritic segments (image composed of micrographs at different focal planes), with 20 μm zoom detailed on the right panel; scale bars = 20 μm. (**a–d**) values ± s.e.m. of total spine densities in basal, apical proximal and apical distal portions of the dendrites from neurons in lesion and peri-lesion sites at 2 (**a** and **c**) and 6 (**c** and **d**) days post injection of aCSF (CON) or L-AA (AA).

mPFC. The function of the mPFC was tested using behavior tasks that rely on this area to assess the impact of the astrocyte pathology and consequent neuronal damage in the computation of cognitive outputs. Astrocyte pathology in the mPFC affects the attentional set-shifting, the working memory and the reversal learning functions. The attentional set-shifting, defined as the capability to 'unlearn' an established contingency in order to learn a new one by shifting the attention from previously irrelevant one to previously salient stimulus is computed by the mPFC in rodents[56] and primates.[68,69] AA animals showed increased difficulty when learning to discriminate the reward pot when indicated by textures in the transition from SDO to SDT stage. This shift of stimuli dimensions—from odor to texture—was shown to be dependent on the intact function of the prelimbic cortex,[70] which, in these animals, was targeted by the L-AA injections. In addition, astrocyte pathology caused a worse performance in the reversal learning stages, which was already described to arise after lesions in the mPFC[71] and might be due to an impairment in the ability to attend relevant stimuli features within the same dimension.[72] These observations are consistent with the critical role displayed by mPFC in shifting to new strategies or rules.[73–76] When tested in water maze tasks, AA animals displayed impaired working memory, which is a cognitive function dependent on the mPFC.[76] Altogether, these behavior data indicate that the astrocyte pathology is sufficient to induce an impairment of the mPFC function. On the basis of the description of similar performances in previous neuronal lesion studies,[56,70,77] this evidence suggests that the behavior impairments observed may be caused mainly by an indirect neuronal degeneration as a consequence of the initial affection of neighbor astrocytes. Until now, we have implicated the poorer performance of the mPFC in the compromised neuronal function as a consequence of surrounding astrocyte pathology, which leads to failure in metabolic supply to neurons,[78,79] homeostasis of K^+ and H^+ ions[3] and neurotransmitters.[1,2,79,80] We should, however, stress that besides these functions, astrocytes are also implicated in the modulation of the synaptic transmission and integration of neuron-glia circuits.[5–7] Although this model is not adequate to assess specifically the function of the tripartite synapse,[5] results presented here indicate a crucial impairment of the network output. As there is still a large group of resilient neurons in the mPFC, we suggest that the lack of astrocytic surveillance in the mPFC synaptic connections may account for network dysfunction and consecutive deficient behavior output.

This study strongly supports the view that astrocytes, targeted in a pathological process, may lead to neurodegeneration in a specific brain region. In the case of mood disorders such as depression or bipolar disorder reported in the literature with impact on cognitive function,[29–40] the changes of astrocytes within the PFC may underlie the cognitive dysfunction observed in these patients.

CONFLICT OF INTEREST

The authors declare no conflict of interest.

ACKNOWLEDGMENTS

This work was supported by the Marie Curie Fellowship FP7-PEOPLE-2010-IEF 273936, BIAL Foundation Grants 138/2008 and 61/2010, FEDER funds through Operational program for competitiveness factors—COMPETE –, ON2 Programa Operacional Regional do Norte (ON.2—O Novo Norte), QREN/FEDER, and by national funds through FCT—Foundation for Science and Technology—project (PTDC/SAU-NSC/118194/2010) and fellowships (SFRH/BPD/66151/2009 and SFRH/BD/89714/2012).

REFERENCES

1 Wang D, Bordey A. The astrocyte odyssey. *Prog Neurobiol* 2008; **86**: 342–367.
2 Parpura V, Heneka MT, Montana V, Oliet SHR, Schousboe A, Haydon PG *et al.* Glial cells in (patho)physiology. *J Neurochem* 2012; **121**: 4–27.
3 Kimelberg HK. Supportive or information-processing functions of the mature protoplasmic astrocyte in the mammalian CNS? A critical appraisal. *Neuron Glia Biol* 2007; **3**: 181–189.
4 Parpura V, Verkhratsky A. Homeostatic function of astrocytes: Ca^{2+} and Na^{+} signalling. *Transl Neurosci* 2012; **3**: 334–344.
5 Araque A, Parpura V, Sanzgiri RP, Haydon PG. Tripartite synapses: glia, the unacknowledged partner. *Trends Neurosci* 1999; **22**: 208–215.
6 Newman EA. New roles for astrocytes: Regulation of synaptic transmission. *Trends Neurosci* 2003; **26**: 536–542.
7 Perea G, Navarrete M, Araque A. Tripartite synapses: astrocytes process and control synaptic information. *Trends Neurosci* 2009; **32**: 421–431.
8 Yang Y, Ge W, Chen Y, Zhang Z, Shen W, Wu C *et al.* Contribution of astrocytes to hippocampal long-term potentiation through release of D-serine. *Proc Natl Acad Sci USA* 2003; **100**: 15194–15199.
9 Perea G, Araque A. Astrocytes potentiate transmitter release at single hippocampal synapses. *Science* 2007; **317**: 1083–1086.
10 Henneberger C, Papouin T, Oliet SHR, Rusakov DA. Long-term potentiation depends on release of D-serine from astrocytes. *Nature* 2010; **463**: 232–236.
11 Florian C, Vecsey CG, Halassa MM, Haydon PG, Abel T. Astrocyte-derived adenosine and A1 receptor activity contribute to sleep loss-induced deficits in hippocampal synaptic plasticity and memory in mice. *J Neurosci* 2011; **31**: 6956–6962.
12 Panatier A, Vallée J, Haber M, Murai KK, Lacaille J-C, Robitaille R. Astrocytes are endogenous regulators of basal transmission at central synapses. *Cell* 2011; **146**: 785–798.
13 Roux L, Benchenane K, Rothstein JD, Bonvento G, Giaume C. Plasticity of astroglial networks in olfactory glomeruli. *Proc Natl Acad Sci* 2011; **108**: 18442–18446.
14 Shigetomi E, Tong X, Kwan KY, Corey DP, Khakh BS. TRPA1 channels regulate astrocyte resting calcium and inhibitory synapse efficacy through GAT-3. *Nat Neurosci* 2011; **15**: 70–80.
15 Woo DH, Han K-S, Shim JW, Yoon B-E, Kim E, Bae JY *et al.* TREK-1 and Best1 channels mediate fast and slow glutamate release in astrocytes upon GPCR activation. *Cell* 2012; **151**: 25–40.
16 Martineau M, Shi T, Puyal J, Knolhoff AM, Dulong J, Gasnier B *et al.* Storage and uptake of D-serine into astrocytic synaptic-like vesicles specify gliotransmission. *J Neurosci* 2013; **33**: 3413–3423.
17 Halassa MM, Florian C, Fellin T, Munoz JR, Lee S-Y, Abel T *et al.* Astrocytic modulation of sleep homeostasis and cognitive consequences of sleep loss. *Neuron* 2009; **61**: 213–219.
18 Di Castro MA, Chuquet J, Liaudet N, Bhaukaurally K, Santello M, Bouvier D *et al.* Local Ca^{2+} detection and modulation of synaptic release by astrocytes. *Nat Neurosci* 2011; **14**: 1276–1284.
19 Takata N, Mishima T, Hisatsune C, Nagai T, Ebisui E, Mikoshiba K *et al.* Astrocyte calcium signaling transforms cholinergic modulation to cortical plasticity *in vivo*. *J Neurosci* 2011; **31**: 18155–18165.
20 Chen N, Sugihara H, Sharma J, Perea G, Petravicz J, Le C *et al.* Nucleus basalis-enabled stimulus-specific plasticity in the visual cortex is mediated by astrocytes. *Proc Natl Acad Sci* 2012; **109**: E2832–E2841.
21 Chen J, Tan Z, Zeng L, Zhang X, He Y, Gao W *et al.* Heterosynaptic long-term depression mediated by ATP released from astrocytes. *Glia* 2013; **61**: 178–191.
22 Han J, Kesner P, Metna-Laurent M, Duan T, Xu L, Georges F *et al.* Acute cannabinoids impair working memory through astroglial CB1 receptor modulation of hippocampal LTD. *Cell* 2012; **148**: 1039–1050.
23 Navarrete M, Perea G, de Sevilla DF, Gómez-Gonzalo M, Núñez A, Martín ED *et al.* Astrocytes mediate *in vivo* cholinergic-induced synaptic plasticity. *PLoS Biol* 2012; **10**: e1001259.
24 Sun W, McConnell E, Pare J-F, Xu Q, Chen M, Peng W *et al.* Glutamate-dependent neuroglial calcium signaling differs between young and adult brain. *Science* 2013; **339**: 197–200.
25 Navarrete M, Perea G, Maglio L, Pastor J, de Sola RG, Araque A. Astrocyte calcium signal and gliotransmission in human brain tissue. *Cereb Cortex* 2013; **23**: 1240–1246.
26 Cotter DR, Pariante CM, Everall IP. Glial cell abnormalities in major psychiatric disorders: the evidence and implications. *Brain Res Bull* 2001; **55**: 585–595.
27 Seifert G, Schilling K, Steinhäuser C. Astrocyte dysfunction in neurological disorders: a molecular perspective. *Nat Rev Neurosci* 2006; **7**: 194–206.
28 Halassa MM, Fellin T, Haydon PG. The tripartite synapse: roles for gliotransmission in health and disease. *Trends Mol Med* 2007; **13**: 54–63.
29 Johnston-Wilson NL, Sims CD, Hofmann JP, Anderson L, Shore AD, Torrey EF *et al.* Disease-specific alterations in frontal cortex brain proteins in schizophrenia, bipolar disorder, and major depressive disorder. The Stanley Neuropathology Consortium. *Mol Psychiatry* 2000; **5**: 142–149.
30 Miguel-Hidalgo JJ, Baucom C, Dilley G, Overholser JC, Meltzer HY, Stockmeier CA *et al.* Glial fibrillary acidic protein immunoreactivity in the prefrontal cortex distinguishes younger from older adults in major depressive disorder. *Biol Psychiatry* 2000; **48**: 861–873.
31 Miguel-Hidalgo JJ, Waltzer R, Whittom AA, Austin MC, Rajkowska G, Stockmeier CA. Glial and glutamatergic markers in depression, alcoholism, and their comorbidity. *J Affect Disord* 2010; **127**: 230–240.
32 Cotter D, Mackay D, Chana G, Beasley C, Landau S, Everall IP. Reduced neuronal size and glial cell density in area 9 of the dorsolateral prefrontal cortex in subjects with major depressive disorder. *Cereb Cortex* 2002; **12**: 386–394.
33 Rajkowska G, Miguel-Hidalgo JJ, Makkos Z, Meltzer H, Overholser J, Stockmeier C. Layer-specific reductions in GFAP-reactive astroglia in the dorsolateral prefrontal cortex in schizophrenia. *Schizophr Res* 2002; **57**: 127–138.
34 Choudary PV, Molnar M, Evans SJ, Tomita H, Li JZ, Vawter MP *et al.* Altered cortical glutamatergic and GABAergic signal transmission with glial involvement in depression. *Proc Natl Acad Sci USA* 2005; **102**: 15653–15658.
35 Webster MJ, O'Grady J, Kleinman JE, Weickert CS. Glial fibrillary acidic protein mRNA levels in the cingulate cortex of individuals with depression, bipolar disorder and schizophrenia. *Neuroscience* 2005; **133**: 453–461.
36 Rajkowska G, Miguel-Hidalgo JJ. Gliogenesis and glial pathology in depression. *CNS Neurol Disord Drug Targets* 2007; **6**: 219–233.
37 Gosselin R-D, Gibney S, O'Malley D, Dinan TG, Cryan JF. Region specific decrease in glial fibrillary acidic protein immunoreactivity in the brain of a rat model of depression. *Neuroscience* 2009; **159**: 915–925.
38 Oh DH, Son H, Hwang S, Kim SH. Neuropathological abnormalities of astrocytes, GABAergic neurons, and pyramidal neurons in the dorsolateral prefrontal cortices of patients with major depressive disorder. *Eur Neuropsychopharmacol J Eur Coll Neuropsychopharmacol* 2012; **22**: 330–338.
39 Cotter DR, Pariante CM, Rajkowska G. Glial Pathology in Major Psychiatric Disorders. In: Agam G, Everall IP, Belmaker RH (eds). *The Postmortem Brain in Psychiatric Research*. Springer: New York, NY, USA, 2002, pp 49–73.
40 Rajkowska G, Stockmeier CA. Astrocyte pathology in major depressive disorder: insights from human postmortem brain tissue. *Curr Drug Targets* 2013; **14**: 1225–1236.
41 Müller N, Schwarz MJ. The immune-mediated alteration of serotonin and glutamate: towards an integrated view of depression. *Mol Psychiatry* 2007; **12**: 988–1000.
42 Klempan TA, Sequeira A, Canetti L, Lalovic A, Ernst C, ffrench-Mullen J *et al.* Altered expression of genes involved in ATP biosynthesis and GABAergic neurotransmission in the ventral prefrontal cortex of suicides with and without major depression. *Mol Psychiatry* 2009; **14**: 175–189.
43 Gómez-Galán M, De Bundel D, Van Eeckhaut A, Smolders I, Lindskog M. Dysfunctional astrocytic regulation of glutamate transmission in a rat model of depression. *Mol Psychiatry* 2013; **18**: 582–594.
44 Hines DJ, Schmitt LI, Hines RM, Moss SJ, Haydon PG. Antidepressant effects of sleep deprivation require astrocyte-dependent adenosine mediated signaling. *Transl Psychiatry* 2013; **3**: e212.
45 Goldman-Rakic PS. Architecture of the prefrontal cortex and the central executive. *Ann N Y Acad Sci* 1995; **769**: 71–83.
46 Davidson RJ. Anxiety and affective style: role of prefrontal cortex and amygdala. *Biol Psychiatry* 2002; **51**: 68–80.
47 Clark L, Cools R, Robbins TW. The neuropsychology of ventral prefrontal cortex: decision-making and reversal learning. *Brain Cogn* 2004; **55**: 41–53.
48 Vertes RP. Differential projections of the infralimbic and prelimbic cortex in the rat. *Synapse* 2004; **51**: 32–58.
49 Heidbreder CA, Groenewegen HJ. The medial prefrontal cortex in the rat: evidence for a dorso-ventral distinction based upon functional and anatomical characteristics. *Neurosci Biobehav Rev* 2003; **27**: 555–579.
50 Hoover WB, Vertes RP. Anatomical analysis of afferent projections to the medial prefrontal cortex in the rat. *Brain Struct Funct* 2007; **212**: 149–179.
51 Banasr M, Duman RS. Glial loss in the prefrontal cortex is sufficient to induce depressive-like behaviors. *Biol Psychiatry* 2008; **64**: 863–870.
52 Banasr M, Chowdhury GMI, Terwilliger R, Newton SS, Duman RS, Behar KL *et al.* Glial pathology in an animal model of depression: reversal of stress-induced cellular, metabolic and behavioral deficits by the glutamate-modulating drug riluzole. *Mol Psychiatry* 2010; **15**: 501–511.

53 Lee Y, Son H, Kim G, Kim S, Lee DH, Roh GS *et al*. Glutamine deficiency in the prefrontal cortex increases depressive-like behaviours in male mice. *J Psychiatry Neurosci* 2013; **38**: 183–191.
54 John CS, Smith KL, Veer AV, Gompf HS, Carlezon WA, Cohen BM *et al*. Blockade of astrocytic glutamate uptake in the prefrontal cortex induces anhedonia. *Neuropsychopharmacology* 2012; **37**: 2467–2475.
55 Khurgel M, Koo AC, Ivy GO. Selective ablation of astrocytes by intracerebral injections of alpha-aminoadipate. *Glia* 1996; **16**: 351–358.
56 Birrell JM, Brown VJ. Medial frontal cortex mediates perceptual attentional set shifting in the rat. *J Neurosci* 2000; **20**: 4320–4324.
57 Morris R. Developments of a water-maze procedure for studying spatial learning in the rat. *J Neurosci Methods* 1984; **11**: 47–60.
58 Cerqueira JJ, Mailliet F, Almeida OFX, Jay TM, Sousa N. The prefrontal cortex as a key target of the maladaptive response to stress. *J Neurosci* 2007; **27**: 2781–2787.
59 Cerqueira JJ, Taipa R, Uylings HBM, Almeida OFX, Sousa N. Specific configuration of dendritic degeneration in pyramidal neurons of the medial prefrontal cortex induced by differing corticosteroid regimens. *Cereb Cortex* 2007; **17**: 1998–2006.
60 Sholl DA. The measurable parameters of the cerebral cortex and their significance in its organization. *Prog Neurobiol* 1956; **2**: 324–333.
61 Uylings HBM, van Pelt J. Measures for quantifying dendritic arborizations. *Network* 2002; **13**: 397–414.
62 Kettenmann H, Hanisch U-K, Noda M, Verkhratsky A. Physiology of Microglia. *Physiol Rev* 2011; **91**: 461–553.
63 Frick LR, Williams K, Pittenger C. Microglial dysregulation in psychiatric disease. *Clin Dev Immunol* 2013; **2013**: 608654.
64 Martin KP, Wellman CL. NMDA receptor blockade alters stress-induced dendritic remodeling in medial prefrontal cortex. *Cereb Cortex* 2011; **21**: 2366–2373.
65 Rothstein JD, Dykes-Hoberg M, Pardo CA, Bristol LA, Jin L, Kuncl RW *et al*. Knockout of glutamate transporters reveals a major role for astroglial transport in excitotoxicity and clearance of glutamate. *Neuron* 1996; **16**: 675–686.
66 Tanaka K, Watase K, Manabe T, Yamada K, Watanabe M, Takahashi K *et al*. Epilepsy and exacerbation of brain injury in mice lacking the glutamate transporter GLT-1. *Science* 1997; **276**: 1699–1702.
67 Selkirk JV, Nottebaum LM, Vana AM, Verge GM, Mackay KB, Stiefel TH *et al*. Role of the GLT-1 subtype of glutamate transporter in glutamate homeostasis: the GLT-1-preferring inhibitor WAY-855 produces marginal neurotoxicity in the rat hippocampus. *Eur J Neurosci* 2005; **21**: 3217–3228.
68 Owen AM, Roberts AC, Polkey CE, Sahakian BJ, Robbins TW. Extra-dimensional versus intra-dimensional set shifting performance following frontal lobe excisions, temporal lobe excisions or amygdalo-hippocampectomy in man. *Neuropsychologia* 1991; **29**: 993–1006.
69 Dias R, Robbins TW, Roberts AC. Primate analogue of the Wisconsin Card Sorting Test: effects of excitotoxic lesions of the prefrontal cortex in the marmoset. *Behav Neurosci* 1996; **110**: 872–886.
70 Ragozzino ME, Detrick S, Kesner RP. Involvement of the prelimbic–infralimbic areas of the rodent prefrontal cortex in behavioral flexibility for place and response learning. *J Neurosci* 1999; **19**: 4585–4594.
71 Kolb B. *The Cerebral Cortex of the Rat*. The MIT Press: Cambridge, MA, US, 1990; 645, p.
72 Bussey TJ, Muir JL, Everitt BJ, Robbins TW. Triple dissociation of anterior cingulate, posterior cingulate, and medial frontal cortices on visual discrimination tasks using a touchscreen testing procedure for the rat. *Behav Neurosci* 1997; **111**: 920–936.
73 De Bruin JP, Sànchez-Santed F, Heinsbroek RP, Donker A, Postmes P. A behavioural analysis of rats with damage to the medial prefrontal cortex using the Morris water maze: evidence for behavioural flexibility, but not for impaired spatial navigation. *Brain Res* 1994; **652**: 323–333.
74 Joel D, Weiner I, Feldon J. Electrolytic lesions of the medial prefrontal cortex in rats disrupt performance on an analog of the Wisconsin Card Sorting Test, but do not disrupt latent inhibition: implications for animal models of schizophrenia. *Behav Brain Res* 1997; **85**: 187–201.
75 Ragozzino ME, Wilcox C, Raso M, Kesner RP. Involvement of rodent prefrontal cortex subregions in strategy switching. *Behav Neurosci* 1999; **113**: 32–41.
76 Kesner RP. Subregional analysis of mnemonic functions of the prefrontal cortex in the rat. *Psychobiology* 2000; **28**: 219–228.
77 Ragozzino ME, Kesner RP. The effects of muscarinic cholinergic receptor blockade in the rat anterior cingulate and prelimbic/infralimbic cortices on spatial working memory. *Neurobiol Learn Mem* 1998; **69**: 241–257.
78 Abbott NJ, Ronnback L, Hansson E. Astrocyte-endothelial interactions at the blood-brain barrier. *Nat Rev Neurosci* 2006; **7**: 41–53.
79 Waagepetersen HS, Sonnewald U, Schousboe A. Energy and Amino Acid Neurotransmitter Metabolism in Astrocytes. In: Haydon PG, Parpura V (eds). *Astrocytes in (Patho)Physiology of the Nervous System*. Springer: New York, NY, USA, 2009, pp 177–200.
80 Nedergaard M, Ransom B, Goldman SA. New roles for astrocytes: redefining the functional architecture of the brain. *Trends Neurosci* 2003; **26**: 523–530.

Supplementary Information accompanies the paper on the Molecular Psychiatry website (http://www.nature.com/mp)